Smooth Sliding Control Applied to Prosthetic Legs via Variable High Gain Observer

Alessandro J. Peixoto, Ignácio de A. M. Ricart and Matheus Ferreira dos Reis

Abstract

In this draft note, we focused on the state estimation of a robot/prosthesis control system with vertical hip displacement, thigh angle and knee angle. The ankle joint is disregarded just to simplify the presentation of the key idea. The dynamic model and the motivation for state estimation were inspired from [1]–[4], where it was mentioned that there are several drawbacks regarding the usage of load cells and/or sensors in robots and prosthetic legs to capture gait data, external forces (GRFs) and moments during walking. Thus, state estimation via Extended Kalman Filter (EKF) [1], [5], High Gain Observer (HGO) [6]–[8] and Sliding Mode Observer (SMO) are promising as well as the estimation of forces acting on the prosthetic foot. We propose the implementation of an HGO with variable dynamic gain. The key idea is to design a time-varying HGO gain synthesized from measurable signals. This dynamic gain can be designed to: (i) reduce the amount of noise in the control signal while keeping an acceptable tracking error transient performance; (ii) guarantee global/semi-global stability properties of the closed-loop system. The main focus is given to the HGO design while the smooth sliding control scheme is left for a future draft of this note.

I. Preliminaries

The following notations and terminology are used:

- The 2-norm (Euclidean) of a vector x and the corresponding induced norm of a matrix A are denoted by $|x|$ and $|A|$, respectively. The symbol $\lambda[A]$ denotes the spectrum of A and $\lambda_m[A] = -\max_i\{Re\{\lambda[A]\}\}$.
- The $\mathscr{L}_{\infty e}$ norm of a signal $x(t) \in \mathbb{R}^n$ is defined as $\|x_t\| := \sup_{0\leq\tau\leq t}|x(\tau)|$.
- The symbol "s" represents either the Laplace variable or the differential operator "d/dt", according to the context.
- As in [9] the output y of a linear time invariant (LTI) system with transfer function $H(s)$ and input u is given by $y = H(s)u$. Convolution operations $h(t) * u(t)$, with $h(t)$ being the impulse response from $H(s)$, will be eventually written, for simplicity, as $H(s) * u$.
- Classes of $\mathscr{K}, \mathscr{K}_\infty$ functions are defined according to [10, p. 144]. ISS, OSS and IOSS mean Input-State-Stable (or Stability), Output-State-Stable (or Stability) and Input-Output-State-Stable, respectively [11].
- The symbol π denotes class-$\mathscr{KL}$ functions. Eventually, we denote by $\pi(t)$ any exponentially decreasing signal, i.e., a signal satisfying $|\pi(t)| \leq \Pi(t)$, where $\Pi(t) := Re^{-\lambda t}$, $\forall t$, for some scalars $R, \lambda > 0$.

II. System Model

The dynamics of the machine/prosthesis system composed by a 3-link rigid body robot[1] with prismatic-revolute-revolute (PRR) configuration, following the notation in [4], is given by:

$$D(q)\ddot{q} + C(q,\dot{q})\dot{q} + B(q,\dot{q}) + P(\dot{q}) + J_e^T F_e + g(q) = F_a\,, \tag{1}$$

where $q^T = \begin{bmatrix} q_1 & q_2 & q_3 \end{bmatrix}$ is the vector of joint displacements (q_1 is the vertical displacement, q_2 is the thigh angle and q_3 is the knee angle), $D(q)$ is the inertia matrix, $C(q,\dot{q})$ is the matrix of Coriolis and centrifugal forces, $B(q,\dot{q})$ is the knee damper nonlinear matrix, J_e is the kinematic Jacobian relative to the point of application of external forces F_e, $g(q)$ is the term of gravitational forces and F_a is the torque/force produced by the actuators. Here, in contrast to [4], we have included the term $P(\dot{q})$ in order to take explicitly into account the Coulomb friction as in [12]. Note that, inertial and frictional effects in the actuators can be included in this model.

To establish a basis for dynamic model derivations and to verify the leg geometry during simulations, the set of reference frames used for forward kinematics problems are the same as the ones assigned in [4]. Matrices $D(q)\ddot{q}$, $C(q,\dot{q})$ and $g(q)$ are obtained using the standard Newton-Euler/Euler-Lagrange approach and are given in Appendix A with the plant parameters extracted from [4].

A. A Simplified Model

In order to illustrate the observer design proposed in this note, consider a simplified version of the machine/prosthesis system (2) where no external forces are considered ($F_e \equiv 0$), the specific leg prosthesis damping matrix is disregarded ($B(q,\dot{q}) \equiv 0$) and the Coulomb friction is neglected ($P(\dot{q}) \equiv 0$). In this case, the machine/prosthesis system is described by:

$$D(q)\ddot{q} + C(q,\dot{q})\dot{q} + g(q) = F_a\,. \tag{2}$$

[1]A more general framework with a n-link rigid body robot can also be considered. However, in order to keep this note close to [4], for simplicity, we have set $n = 3$.

The system matrices $D(q), C(q,\dot{q})$ and $g(q)$ are supposed to be uncertain, but the corresponding nominal matrices $D_n(q), C_n(q,\dot{q})$ and $g_n(q)$ are assumed known. In particular, the inertia matrix $D(q)$ which is invertible, since $D(q) = D^T(q)$ is strictly positive definite.

Introducing the variables $x_1 := q \in \mathbb{R}^3$ and $x_2 := \dot{q} \in \mathbb{R}^3$, the model (2) can be rewritten in the state-space form as:

$$\dot{x}_1 = x_2, \tag{3}$$
$$\dot{x}_2 = k_p(x,t)\,[u + d(x,t)], \quad u := F_a \in \mathbb{R}^{3\times 1}, \tag{4}$$
$$y = x_1, \tag{5}$$

or, equivalently,

$$\dot{x} = A_\rho x + B_\rho k_p(x,t)[u + d(x,t)], \tag{6}$$
$$y = C_\rho x, \tag{7}$$

where $x^T = \left[\begin{array}{cc} x_1 & x_2 \end{array}\right]$ is the state vector, $k_p(x,t) = D(x_1)^{-1} \in \mathbb{R}^{3\times 3}$, $d(x,t) := -C(x_1,x_2)x_2 - g(x_1) \in \mathbb{R}^{3\times 1}$, $C_\rho = \left[\begin{array}{cc} I_{3\times 3} & 0_{3\times 3} \end{array}\right] \in \mathbb{R}^{3\times 6}$ and the pair (A_ρ, B_ρ) is in Brunovskys canonical controllable form and is given by:

$$A_\rho = \left[\begin{array}{cc} 0_{3\times 3} & I_{3\times 3} \\ 0_{3\times 3} & 0_{3\times 3} \end{array}\right] \in \mathbb{R}^{6\times 6},$$

and

$$B_\rho = \left[\begin{array}{cc} 0_{3\times 3} & I_{3\times 3} \end{array}\right]^T \in \mathbb{R}^{6\times 3}.$$

For each solution of (6) there exists a maximal time interval of definition given by $[0, t_M)$, where t_M may be finite or infinite. Thus, finite-time escape is not precluded, *a priori*.

Remark. (**Nominal Values**) Nominal terms can be used in the HGO implementation in order to reduce conservatism in the HGO design. The plant could be rewritten as:

$$\dot{x}_1 = x_2, \tag{8}$$
$$\dot{x}_2 = f(x_1,x_2,u,t) + \delta_f(x_1,x_2,u,t), \quad u := F_a, \tag{9}$$
$$y = x_1, \tag{10}$$

where the nominal part of the system dynamics is represented by

$$f(x_1,x_2,u,t) := D_n^{-1}(x_1)u - D_n^{-1}(x_1)\left[C_n(x_1,x_2)x_2 + g_n(x_1)\right], \tag{11}$$

while the uncertainties are concentrated in the term

$$\delta_f(x_1,x_2,u,t) := \left[D^{-1}(x_1) - D_n^{-1}(x_1)\right]u + \left[D_n^{-1}(x_1)C_n(x_1,x_2) - D^{-1}(x_1)C(x_1,x_2)\right]x_2 + D_n^{-1}(x_1)g_n(x_1) - D^{-1}(x_1)g(x_1). \tag{12}$$

However, to simplify this presentation while keeping the main HGO design methodology, consider $C_n \equiv 0$, $g_n \equiv 0$ and, since D is assumed known, we also have $D_n = D$.

III. High Gain Observer with Variable Gain

The HGO [7] is given by

$$\dot{\hat{x}} = A_\rho \hat{x} + B_\rho k_p^n u + H_\mu L_o (y - C_\rho \hat{x}), \tag{13}$$

where k_p^n is a nominal value of the plant high frequency gain (HFG) k_p and L_o and H_μ are given by:

$$L_o = \left[\begin{array}{cc} l_1 I_{3\times 3} & l_2 I_{3\times 3} \end{array}\right]^T \in \mathbb{R}^{6\times 3} \text{ and } H_\mu := \text{diag}(\mu^{-1} I_{3\times 3},\ \mu^{-2} I_{3\times 3}) \in \mathbb{R}^{6\times 6}. \tag{14}$$

The observer gain L_o is such that $s^2 + l_1 s + l_2$ is Hurwitz. In this paper, instead of using a constant μ, we introduce a *variable* parameter $\mu = \mu(t) \neq 0, \forall t \in [0, t_M)$, of the form

$$\mu(\omega,t) := \frac{\bar{\mu}}{1 + \psi_\mu(\omega,t)}, \tag{15}$$

where ψ_μ, named **adapting function**, is a non-negative function continuous in its arguments and ω is an available signal, both to be designed later on. The parameter $\bar{\mu} > 0$ is a design constant. For each system trajectory, μ is absolutely continuous and $\mu \leq \bar{\mu}$. Note that μ is bounded for t in any finite sub-interval of $[0, t_M)$. Therefore,

$$\mu(\omega,t) \in [\underline{\mu}, \bar{\mu}], \quad \forall t \in [t_*, t_M), \tag{16}$$

for some $t_* \in [0, t_M)$ and $\underline{\mu} \in (0, \bar{\mu})$.

A. High Gain Observer Error Dynamics

The transformation [13]

$$\zeta := T_\mu \tilde{x}, \quad T_\mu := [\mu^2 H_\mu]^{-1} \in \mathbb{R}^{6\times 6}, \quad \tilde{x} := x - \hat{x}, \tag{17}$$

is fundamental to represent the $\tilde{x}$-dynamics in convenient coordinates allowing us to show that $\tilde{x}$ is arbitrarily small, *modulo* exponentially decaying term. First, note that:

$$(i)\ T_\mu(A_\rho - H_\mu L_o C_\rho)T_\mu^{-1} = \frac{1}{\mu}A_o\,, \quad (ii)\ T_\mu B_\rho = B_\rho\,, \quad \text{and} \quad (iii)\ \dot{T}_\mu T_\mu^{-1} = \frac{\dot{\mu}}{\mu}\Delta,$$

where $A_o := A_\rho - L_o C_\rho$ and $\Delta := \mathrm{diag}(-I_{3\times 3},\ 0_{3\times 3}) \in \mathbb{R}^{6\times 6}$. Then, subtracting (13) from (6) and applying the above relationships (i), (ii) and (iii), the dynamics of $\tilde{x}$ in the new coordinates ζ (17) is given by:

$$\mu\dot{\zeta} = [A_o + \dot{\mu}(t)\Delta]\zeta + B_\rho[\mu\nu]\,, \tag{18}$$

where

$$\nu := (k_p - k_p^n)u + k_p d\,, \tag{19}$$

and

$$\dot{\mu}(t) = -\frac{\mu^2}{\bar{\mu}}\left[\frac{\partial\psi_\mu}{\partial\omega}\dot{\omega} + \frac{\partial\psi_\mu}{\partial t}\right]. \tag{20}$$

The HGO gain ($H_\mu L_o$) is inversely proportional to the small parameter μ, allowed to be time-varying. Our task is to establish properties for the adapting function $\psi_\mu(\omega,t)$ in (15) so that $\mu|\nu|$ and $|\dot{\mu}|$ are arbitrarily small, at least after a finite time interval. In fact, we design ψ_μ so that the following inequalities hold

$$|\dot{\mu}(t)|,\ \mu|\nu| \le \mathscr{O}(\bar{\mu}), \quad \forall t \in [t_\mu, t_M). \tag{21}$$

for some finite $t_\mu \in [0, t_M)$. Consequently, $\dot{\mu}$ does not *ultimately* affect the stability of A_o in (18) and ζ can be made arbitrarily small, *modulo* an exponentially decaying term, by applying a time scale changing in (18). In addition, since $\tilde{x} = T_\mu^{-1}\zeta$ and $\|T_\mu^{-1}\|$ is of order $\mathscr{O}(1)$, then one can conclude that $\tilde{x}$ can also be made arbitrarily small, *modulo* an exponentially decaying term.

It is clear that inequalities in (21) depend on the choice of the control signal u in (19), the disturbance and the signal ω.

B. The Adapting Function ψ_μ

The adapting function $\psi_\mu(\omega,t)$ used in the time-varying parameter

$$\mu(\omega,t) := \frac{\bar{\mu}}{1+\psi_\mu(\omega,t)}\,, \tag{22}$$

defined in (15), can assume different forms depending on the choice of the signal ω and the available information about the plant.

As an example, consider the following cases:

1) **From a theoretical point of view**: the adapting function ψ_μ can be chosen in order to allow global/semi-global stability (or only convergence) properties for the closed-loop control system.
   a) **Norm Observability**: The plant (6)–(7) admits a norm observer which provides an upper bound for the plant state norm by using only available signals: plant input (u) and plant output (y). In this case, global or semi-global results could be obtained when, for example, a sliding mode based control is employed, as in [14].
   More precisely, a norm observer for system (6)–(7) is a m-order dynamic system of the form:

$$\tau_1\dot{\omega}_1 = -\omega_1 + u\,, \tag{23}$$

$$\tau_2\dot{\omega}_2 = \gamma_o(\omega_2) + \tau_2\varphi_o(\omega_1, y, t)\,, \tag{24}$$

   with states $\omega_1 \in \mathbb{R}$, $\omega_2 \in \mathbb{R}^{m-1}$ and positive constants τ_1, τ_2 such that for $t \in [0, t_M)$: (i) if $|\varphi_o|$ is uniformly bounded by a constant $c_o > 0$, then $|\omega_2|$ can escape at most exponentially and there exists $\tau_2^*(c_o)$ such that the ω_2-dynamics is BIBS (Bounded-Input-Bounded-State) stable w.r.t. φ_o for $\tau_2 \le \tau_2^*$; (ii) for each $x(0), \omega_1(0), \omega_2(0)$, there exists $\bar{\varphi}_o$ such that

$$|x(t)| \le \bar{\varphi}_o(\omega(t),t) + \pi_o(t)\,, \quad \omega := [\omega_1\ \ \omega_2^T\ \ y]^T\,, \tag{25}$$

   where $\pi_o := \beta_o(|\omega_1(0)| + |\omega_2(0)| + |x(0)|)e^{-\lambda_o t}$ with some $\beta_o \in \mathscr{K}_\infty$ and positive constant λ_o.
   b) **The system states can be assumed bounded**: The plant state, in particular the unavailable state x_2, is uniformly bounded. Such assumption of the state boundedness is true, for example, when (6) is BIBS stable, and the control

input is bounded. Moreover, by considering that the acceleration ($\dot{x}_2$) in the mechanical system is bounded by a known constant, then a constant upper bound for the velocity x_2 can be found by using the "dirty derivative":

$$\eta := \frac{\tau}{\tau s+1} y. \tag{26}$$

Indeed, by noting that

$$x_2 = \eta + \frac{\tau}{\tau s+1}\dot{x}_2\,, \tag{27}$$

one can obtain the following norm bound

$$|x_2| \leq |\eta| + \mathscr{O}(\tau)\|\dot{x}_2\|\,.$$

In this case, we can use this rough estimate for x_2 and less conservative estimates for the terms depending on y, so that ω can be implemented.

2) **From a practical point of view**: one can select a time-varying adapting function ψ_μ to assure an acceptable level of noise in the control signal while keeping a good transient for the output tracking error.

a) **Signal-to-Noise Ratio in $|u|$ $\times$ Tracking Error Norm**: By using some measurement of the amount of noise in the control signal, for example, the Signal-to-Noise Ratio (SNR), the adapting function can be implemented as a function of the SNR and the tracking error, so that μ increases when the SNR in the control effort increases and μ decreases when the tracking error norm increases. This can be accomplished, for example, by defining a cost function depending on the control signal-to-noise ratio and the output tracking error, so that the time-varying μ reaches an optimum value.

C. One Particular Design for ψ_μ via Domination Techniques

When the plant (6)–(7) admits a norm observer with ω defined in (25) such that

$$|x(t)| \leq \bar{\varphi}_o(\omega(t),t) + \pi_o(t)\,, \tag{28}$$

and a sliding mode based control is employed, then the signal v satisfies (see [14] for details):

$$|v| \leq \psi_v(\omega,t) + \pi_3\,, \tag{29}$$

for some non-negative function ψ_ω and vanishing term π_3 depending on initial conditions. Moreover, the signal ω is such that the following inequality holds (see [14] for details):

$$|\dot{\omega}| \leq \psi_\omega(\omega,t) + \pi_1\,, \tag{30}$$

respectively, for some non-negative functions ψ_ω and vanishing terms π_1 depending on initial conditions. In order to obtain a norm bound for the time derivative of μ (15) we calculate $\dot{\mu}$ by the expression:

$$\dot{\mu}(t) = -\frac{\mu^2}{\bar{\mu}}\left[\frac{\partial \psi_\mu}{\partial \omega}\dot{\omega} + \frac{\partial \psi_\mu}{\partial t}\right]. \tag{31}$$

Note that, $\dot{\mu}$ is a piecewise continuous time signal which can be upperbounded by

$$|\dot{\mu}(t)| \leq \frac{\left|\frac{\partial \psi_\mu}{\partial \omega}\right|}{1+\psi_\mu}\mu|\dot{\omega}| + \frac{\left|\frac{\partial \psi_\mu}{\partial t}\right|}{1+\psi_\mu}\mu\,. \tag{32}$$

Hence, one has that:

$$\mu|v| \leq \frac{\psi_v}{1+\psi_\mu}\bar{\mu} + \mu\pi_3\,, \tag{33}$$

and

$$\mu|\dot{\omega}| \leq \frac{\psi_\omega}{1+\psi_\mu}\bar{\mu} + \mu\pi_1\,. \tag{34}$$

Now, choose the adapting function ψ_μ in (15) so that the following property holds with ψ_v in (29) and ψ_ω in (30):

(P0) $\psi_v\,,\ \psi_\omega \leq c_{\mu 0}(1+\psi_\mu)$, $\forall t \in [0,t_M)$, where $c_{\mu 0} \geq 0$ is a *known* constant.

If ψ_μ satisfies (P0) then, from (33) and (34), $\mu|v|$ and $\mu|\dot{\omega}|$ can be bounded by

$$\mu|v| \leq \mathscr{O}(\bar{\mu}) + \mu\pi_3\,. \tag{35}$$

$$\mu|\dot{\omega}| \leq \mathscr{O}(\bar{\mu}) + \mu\pi_1\,. \tag{36}$$

Moreover, our strategy is to design $\psi_\mu(\omega,t)$ such that the following property holds:

(P1) $\left|\frac{\partial \psi_\mu}{\partial \omega}\right|, \left|\frac{\partial \psi_\mu}{\partial t}\right| \leq c_{\mu 1}(1+\psi_\mu)$, $\forall t \in [0, t_M)$, where $c_{\mu 1} \geq 0$ is a *known* constant.

This property is trivially satisfied by polynomial ψ_μ with positive coefficients. Now, with ψ_μ satisfying (P1), one has that:

$$|\dot{\mu}(t)| \leq c_{\mu 1}\mu|\dot{\omega}| + c_{\mu 1}\mu\,. \tag{37}$$

Therefore, from (37), (35) and (36) the following holds:

$$|\dot{\mu}(t)|,\ \mu|\nu| \leq \mathscr{O}(\bar{\mu}) + \mu\pi_4\,, \tag{38}$$

where $\pi_4 := c_{\mu 1}\pi_1 + \pi_3$.

Finally, if ψ_μ is designed so that (P0)–(P1) hold and *finite escape is avoided*[2], then from (38) one can verify that there exists a finite $t_\mu \in [0, t_M)$ such that:

$$|\dot{\mu}(t)|,\ \mu|\nu| \leq \mathscr{O}(\bar{\mu}), \quad \forall t \in [t_\mu, t_M)\,. \tag{39}$$

In this case, the stability and/or convergence analysis can be carried out by noting that the output tracking error dynamics (and the full error system dynamics) is ISS w.r.t. HGO estimate error $\tilde{x}$ which is of order $\mathscr{O}(\bar{\mu})$ after the small finite time instant t_μ.

IV. Numerical Simulations

The control objective is to reduce the tracking error

$$e(t) := y_d - y\,, \tag{40}$$

where the desired trajectory is defined as:

$$y_d(t) := \begin{bmatrix} 0.02\cos\left(\frac{2\pi}{0.55}t\right) & 0.9\sin\left(\frac{2\pi}{1.5}t\right)+1 & \sin\left(\frac{2\pi}{0.45}t\right)+1.8 \end{bmatrix}^T. \tag{41}$$

The reference trajectory was defined in order to approximate the desired trajectories appearing in [4]. For simplicity, the time-varying derivatives ($\dot{y}_d$ and $\ddot{y}_d$) were obtained by using a "dirty derivative" of the desired trajectory y_d. The plant initial conditions are: $y(0) = x_1(0) = \begin{bmatrix} 0 & \pi/4 & \pi/4 \end{bmatrix}^T$ and $x_2(0) = \begin{bmatrix} 0 & 0 & 0 \end{bmatrix}^T$.

A simple PD controller with feedforward is employed just to validate the time-varying HGO proposed in this note. By recalling that we consider $D_n(y) = D(y)$ to simplify the paper presentation, the control signal is given by

$$u(t) := D(y)u_v + C_n(y,\hat{x}_2)\hat{x}_2 + g_n(y)\,, \tag{42}$$

$$u_v(t) := \ddot{q}_d + K_p e(t) + \underbrace{K_d(\dot{y}_d - \hat{x}_2)}_{\approx K_d \frac{de(t)}{dt}}\,, \tag{43}$$

where $\hat{x}_2$ is the estimate for x_2 obtained from the HGO and

$$K_p = K_d = \begin{bmatrix} 10 & 0 & 0 \\ 0 & 10 & 0 \\ 0 & 0 & 10 \end{bmatrix}.$$

Note that, in the ideal case when the nominal matrices C_n and g_n match the real values and $\hat{x}_2 = x_2$, the following closed-loop equation holds

$$\ddot{e} + K_d\dot{e} + K_p e = 0\,, \tag{44}$$

which assures that $|e(t)| \to 0$ as $t \to \infty$. When there are uncertainties in the plant parameters and/or errors in the HGO estimate, the tracking error converges to some residual set. The nominal matrix D_n is given by (46) replacing: I_2 by I_2^n, C_2 by C_2^n, C_3 by C_3^n and m_1, m_2, m_3 by m_1^n, m_2^n, m_3^n, respectively, where $I_2^n, C_2^n, C_3^n, m_1^n, m_2^n$ and m_3^n are the "known" nominal values of the parameters given in Table I. The nominal value of the HFG is given by $k_p^n = D_n^{-1}$. The nominal matrix C_n is given by (45) replacing: C_2 by C_2^n, C_3 by C_3^n and m_1, m_2, m_3 by m_1^n, m_2^n, m_3^n, respectively. The nominal matrix g_n is given by (47) replacing m_1, m_2, m_3 by m_1^n, m_2^n, m_3^n, respectively.

The *actual* plant parameters, assumed partially unknown, are given in Table II. We consider that the real parameters differ from the known values by not more than 1% or 5%.

The HGO is implemented with $l_1 = 2$, $l_2 = 1$ and with a constant $\mu = \bar{\mu} = 0.01$. Fig. 1 depicts the hip displacement and its estimation via HGO converging before 20ms with an undershoot less than 0.01 meters. A similar behavior for the thigh and knee angle can be observed in Fig. 2 and Fig. 3, respectively, with their HGO estimates. Both estimates converge before 15ms with transient error less than 0.4rad (approximately 22^o). The corresponding hip, thigh and knee velocities are illustrated in Fig. 4, Fig. 5 and Fig. 6, respectively.

TABLE I

NOMINAL VALUES.

Parameter	Value	Units
m_1^n, m_2^n, m_3^n	+1% error w.r.t. m_1, m_2, m_3	Kg
C_2^n	+5% error w.r.t. C_2	m
C_3^n	-5% error w.r.t. C_3	m
I_2^n	-5% error w.r.t. I_2	$Kg\ m^2$

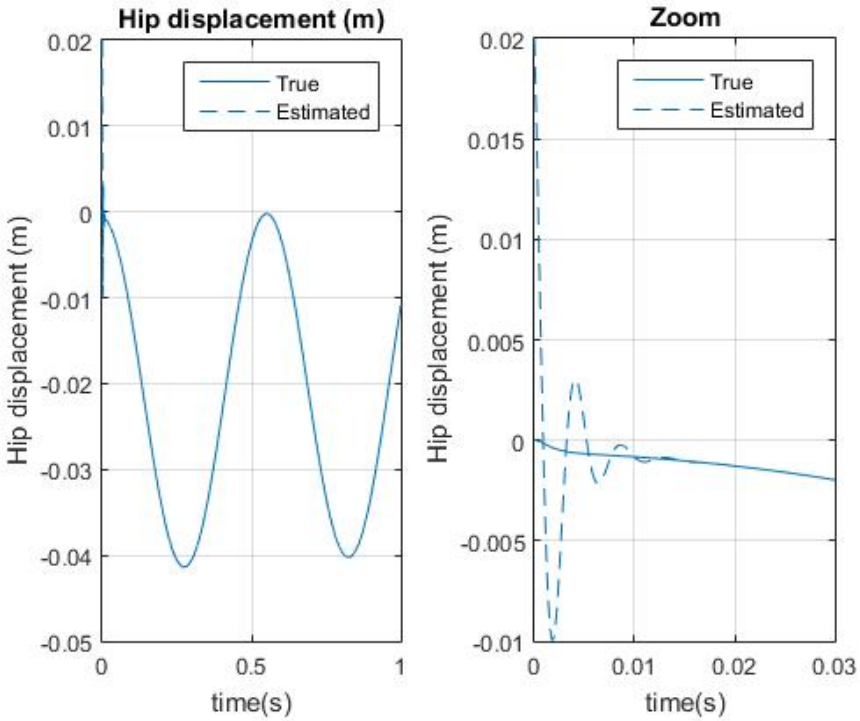

Fig. 1. Hip displacement. Simulation results with PD control with feedforward and HGO with constant parameter $\mu = 0.01$.

Now, in order to illustrate one possible scenario in which the time-varying HGO parameter can be used, consider that the plant parameters are known and that the HGO is implemented to obtain an estimate for the state x_2.

In order to observe the effect of the input disturbance, a large but unknown constant input disturbance is employed at $t = 3$, vanishing at $t = 10$, with small plant initial conditions $y(0) = x_1(0) = \begin{bmatrix} 0 & \pi/36 & 0 \end{bmatrix}^T$ and $x_2(0) = \begin{bmatrix} 0 & 0 & 0 \end{bmatrix}^T$. Since no integral action is implemented in the control scheme, the input disturbance causes a considerable large transient in the tracking error. This transient increases as μ increases and it is useful to illustrate the usage of the time-varying parameter μ.

By applying a constant and large value of $\mu(t) = \bar{\mu} = 0.1$ an apparent degradation in the closed-loop tracking error transient is observed in Fig. 7 (a). On the other hand, the noise amplitude in the control signal is acceptable as can be observed in Fig. 7 (b) with the corresponding measurement of the noise amplitude illustrated in Fig. 7 (c). The noise amplitude was obtained by filtering the control input u with a high-pass filter. By reducing μ to the constant small value $\mu(t) = \bar{\mu} = 0.01$, the tracking error transient is improved in exchange of an increase on the control signal noise, see Fig. 8 (a), (b) and (c). On the other hand, when the time-varying $\mu(t)$ is implemented starting with the same large value for $\bar{\mu} = 0.1$, the tracking error transient is improved, see Fig. 9 (a), without reducing μ to a prohibitive value which can cause a large noise in the control signal, as illustrated in Fig. 9 (b) and (c). In this case, the time evolution of $\mu(t)$ is shown in Fig. 10 (a), from which one can verify that μ reaches a minimum value of $\mu_{min} = 0.02$. This value is not known *a priori*. It is clear that care must be taken while reducing $\bar{\mu}$, since there exists a trade off between noise reduction and tracking accuracy.

V. CONCLUSIONS

In this note, we considered the state estimation problem of a robot/prosthesis control system with vertical hip displacement, thigh angle and knee angle. It was verified that it is possible to apply HGO with dynamic gain in order to reduce the amount

[2]This can be guaranteed if an additional technical Property is satisfied, see [14] for details. Here, we omitted this property just to simplify the paper presentation.

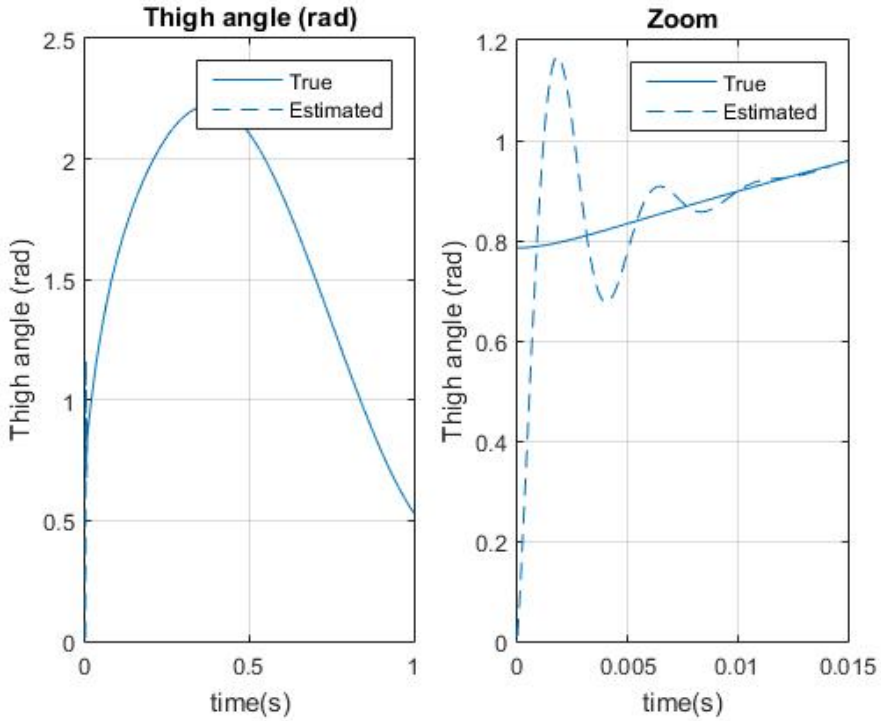

Fig. 2. Thigh angle. Simulation results with PD control with feedforward and HGO with constant parameter $\mu = 0.01$.

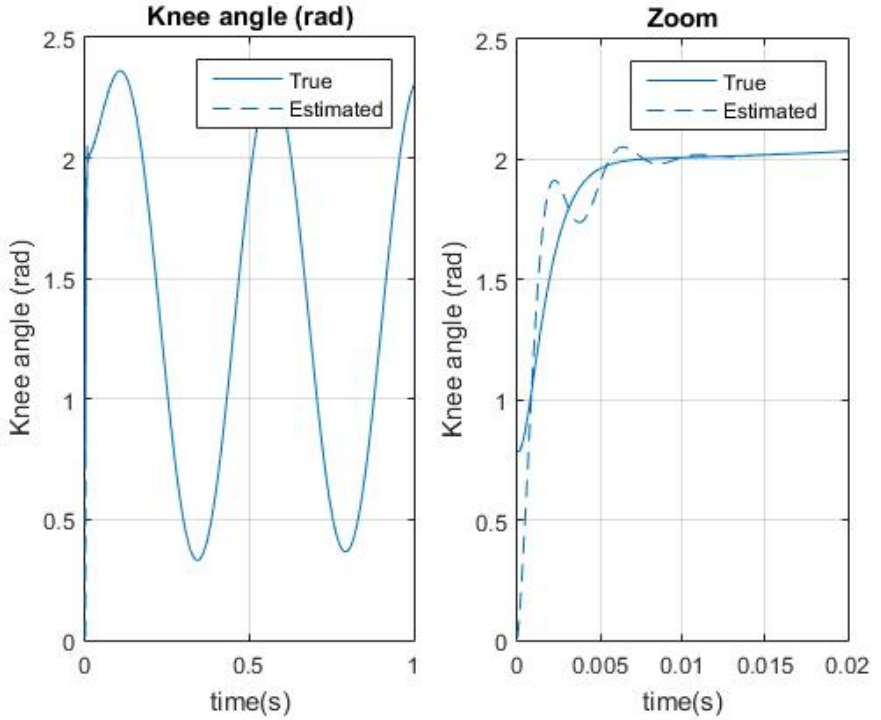

Fig. 3. Knee angle. Simulation results with PD control with feedforward and HGO with constant parameter $\mu = 0.01$.

of noise in the control signal while assuring an reasonable output tracking error transient. Moreover, when a norm observer is available, domination techniques can be used to design the HGO dynamic gain to obtain global/semi-global practical tracking. An illustrative academic simulation example was presented.

Future possible topics of research are: (i) consider the full robot/prosthesis model including the ground reaction forces

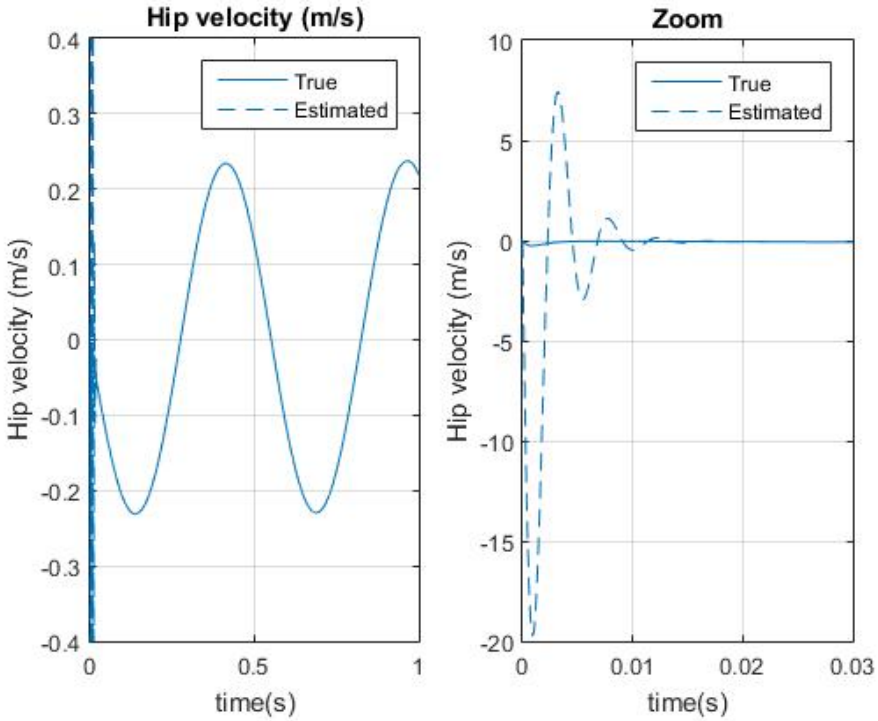

Fig. 4. Hip velocity. Simulation results with PD control with feedforward and HGO with constant parameter $\mu = 0.01$.

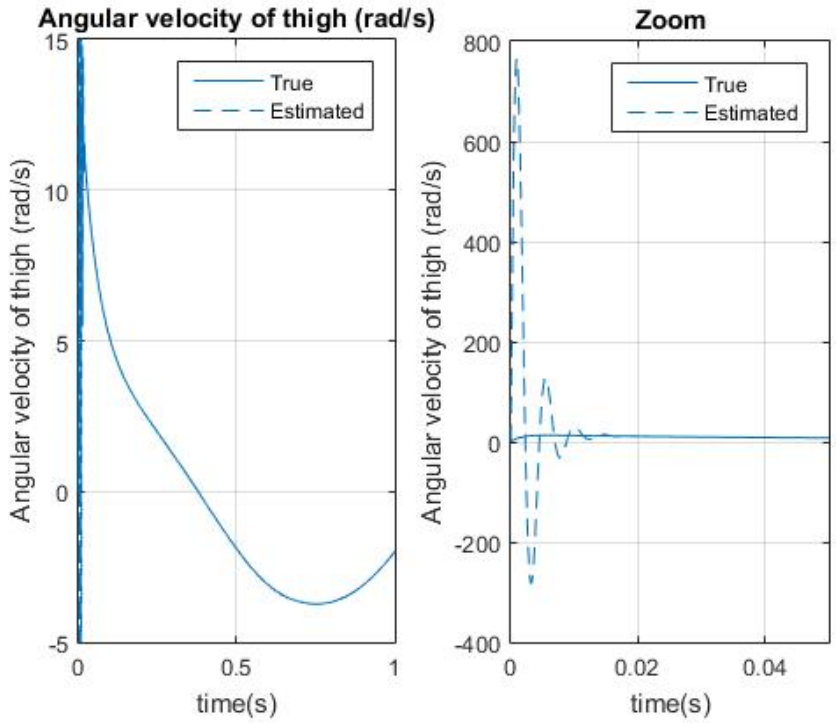

Fig. 5. Thigh angular velocity. Simulation results with PD control with feedforward and HGO with constant parameter $\mu = 0.01$.

and the ankle joint and its estimation; (ii) verify if it is possible to obtain a norm bound for the system state in order to assure global/semi-global stability properties; (iii) design and implementation of the smooth sliding control scheme and (iv) perform experimental results.

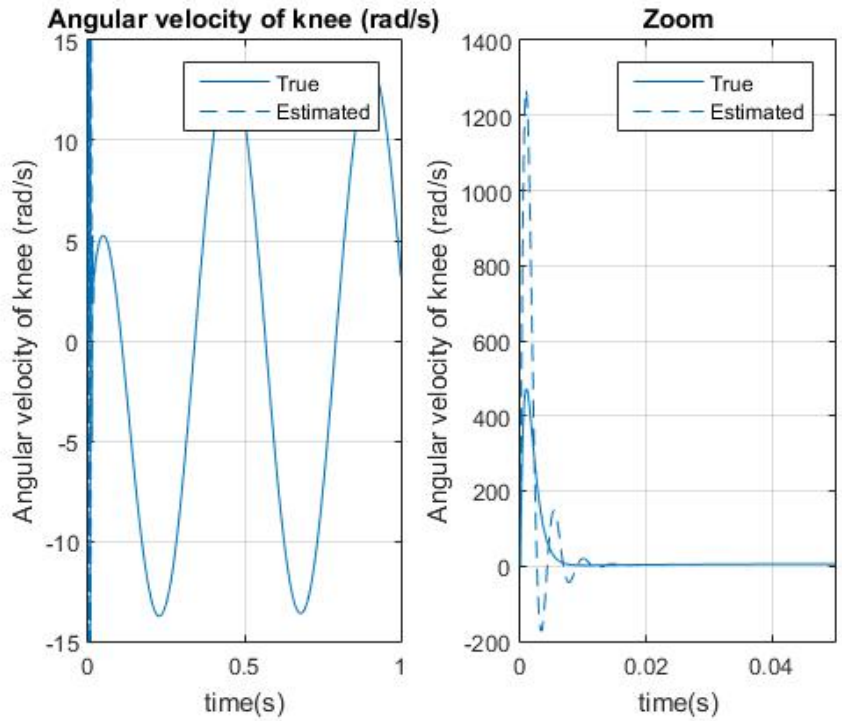

Fig. 6. Knee angular velocity. Simulation results with PD control with feedforward and HGO with constant parameter $\mu = 0.01$.

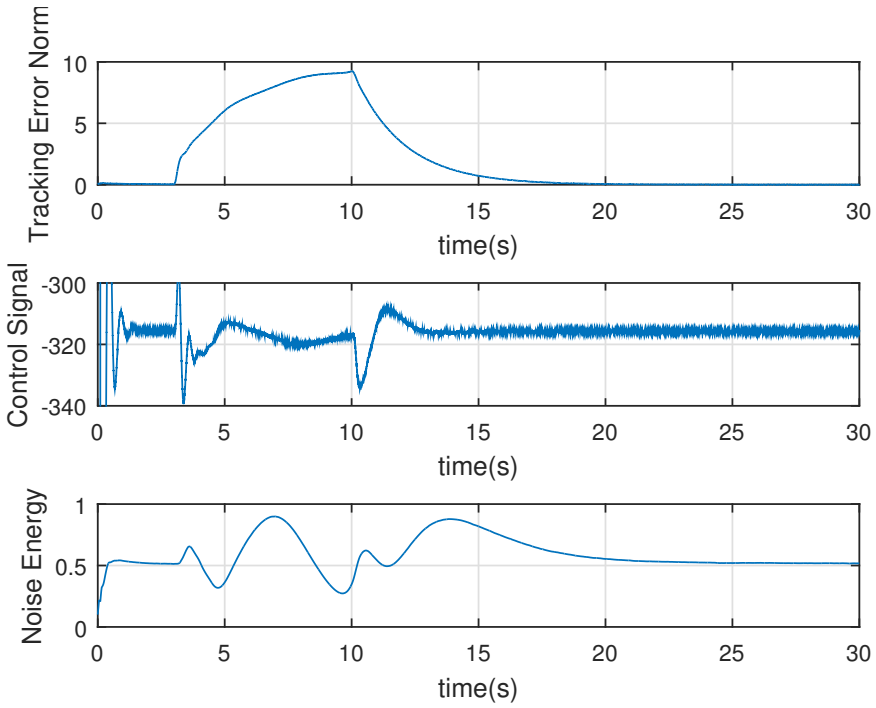

Fig. 7. Simulation results with a constant HGO parameter $\mu(t) = \bar{\mu} = 0.1$.

REFERENCES

[1] S. A. Fakoorian and D. Simon, "Ground reaction force estimation in prosthetic legs with an extended kalman filter," *Systems Conference (SysCon), 2016 Annual IEEE*, pp. 1–6, 2016.

[2] V. Azimi, D. Simon, and H. Richter, "Stable robust adaptive impedance control of a prosthetic leg," *ASME 2015 Dynamic Systems and Control Conference*, vol. 1, pp. 1–10, 2015.

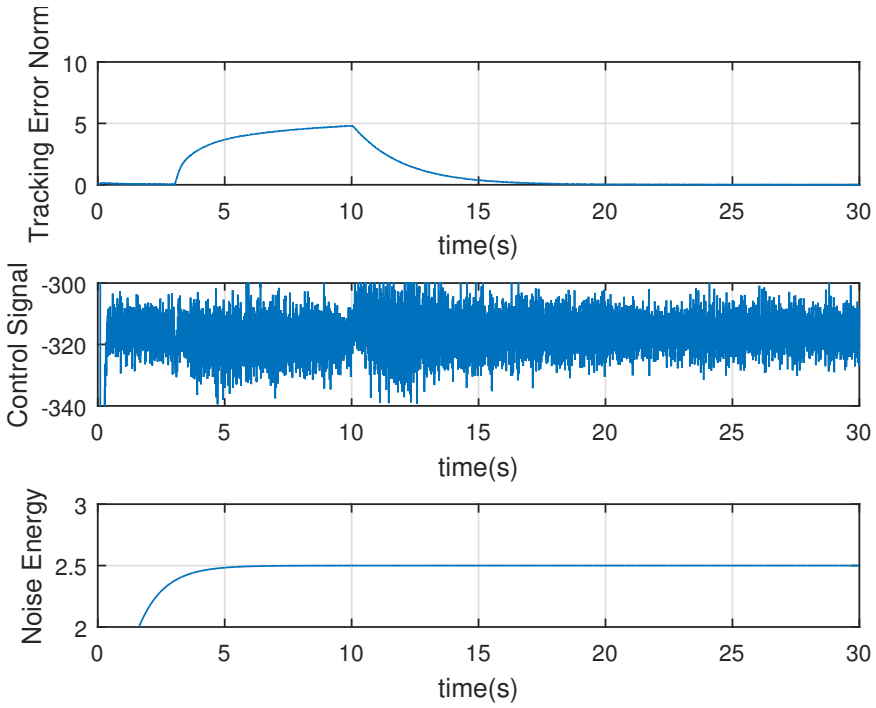

Fig. 8. Simulation results with a constant HGO parameter $\mu(t) = \bar{\mu} = 0.01$.

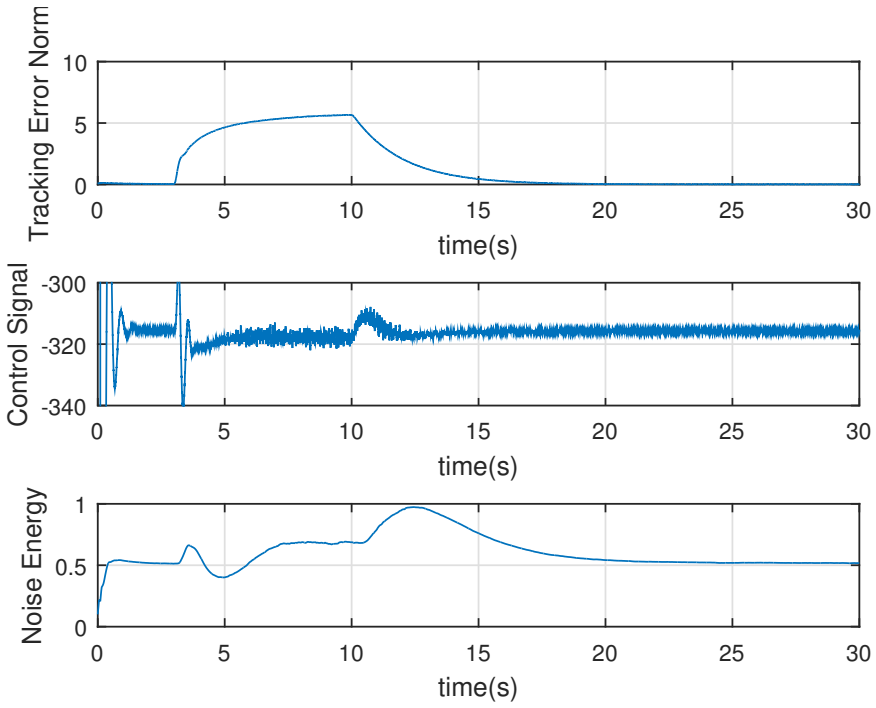

Fig. 9. Simulation results with the time-varying HGO parameter $\mu(t)$.

[3] H. Warner, D. Simon, and H. Richter, "Design Optimization and Control of a Crank-Slider Actuator for a Lower-Limb Prosthesis with Energy Regeneration," *2016 IEEE International Conference on Advanced Intelligent Mechatronics (AIM)*, pp. 1430–1435, 2016.

[4] H. Richter, D. Simon, W. A. Smith, and S. Samorezov, "Dynamic modeling, parameter estimation and control of a leg prosthesis test robot," *Applied Mathematical Modelling*, vol. 39, no. 2, pp. 559–573, 2015.

[5] R. Huang, S. C. Patwardhan, and L. T. Biegler, "Robust output-feedback nonlinear model predictive control using high-gain observers," *10 International*

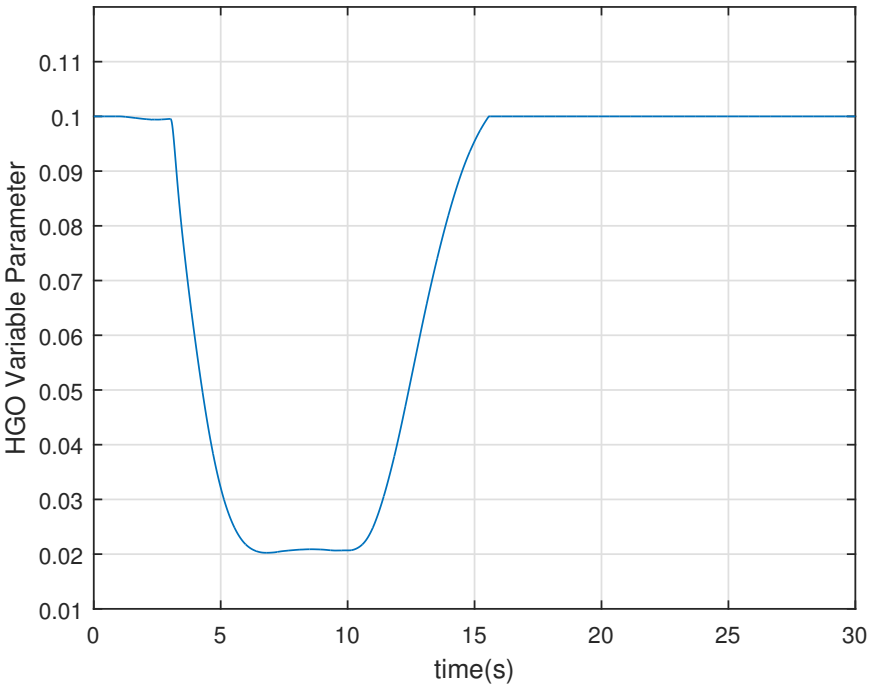

Fig. 10. Simulation results. The time-varying HGO parameter $\mu(t)$.

Symposium on Process Systems Engineering: Part A, vol. 27, pp. 1611 – 1616, 2009.

[6] G. Zhang, J. Gao, W. Yan, and C. Liu, "High-gain observer-based model predictive control for cross tracking of underactuated autonomous underwater vehicles," *2016 IEEE International Conference on Underwater System Technology: Theory and Applications (USYS)*, pp. 115–120, 2016.

[7] H. K. Khalil, "High-gain observers in nonlinear feedback control," *2008 International Conference on Control, Automation and Systems*, pp. xlvii – lvii, 2008.

[8] B. A. Foss, R. Findeisen, L. Imsland, and F. Allgwer, "Output-feedback nonlinear model predictive control using high-gain observers in original coordinates," *2003 European Control Conference (ECC)*, pp. 2014–2019, 2003.

[9] P. Ioannou and J. Sun, *Robust Adaptive Control*. Prentice-Hall, 1996.

[10] H. K. Khalil, *Nonlinear Systems*, 3^{rd} ed. Prentice Hall, 2002.

[11] E. D. Sontag and Y. Wang, "On characterizations of the input-to-state stability property," *Systems & Contr. Letters*, vol. 24, pp. 351–359, 1995.

[12] J. Lee, R. Mukherjee, and H. K. Khalil, "Output feedback stabilization of inverted pendulum on a cart in the presence of uncertainties," *Automatica*, vol. 54, pp. 146–157, 2015.

[13] S. Oh and H. K. Khalil, "Nonlinear output-feedback tracking using high-gain observer and variable structure control," *Automatica*, vol. 33, no. 10, pp. 1845–1856, 1997.

[14] A. J. Peixoto, T. R. Oliveira, and L. Hsu, "Global tracking sliding mode control for a class of nonlinear systems via variable gain observer," *International Journal of Robust and Nonlinear Control*, pp. 177–196, 2011.

APPENDIX

A. System Matrices and Parameters

The plant parameters are given in Table II, while the matrices $D(q), C(q,\dot{q})$ and $g(q)$, appearing in (1), are given by:

$$\begin{aligned}
C(1,1) &= C(2,1) = C(3,1) = C(3,3) = 0\,,\\
C(1,2) &= -\dot{q}_2(L_2m_3 + m_2(C_2 + L_2))\sin(q_2) - C_3m_3(\dot{q}_2 + \dot{q}_3)\sin(q_2 + q_3)\,,\\
C(1,3) &= -C_3m_3\sin(q_2 + q_3)(\dot{q}_2 + \dot{q}_3)\,,\\
C(2,2) &= -C_3L_2m_3\dot{q}_3\sin(q3)\,,\\
C(2,3) &= -C_3L_2m_3\sin(q_3)(\dot{q}_2 + \dot{q}_3)\,,\\
C(3,2) &= C_3L_2m_3\dot{q}_2\sin(q_3)\,,
\end{aligned} \tag{45}$$

$$\begin{aligned}
D(1,1) &= m_1 + m_2 + m_3\,,\\
D(1,2) &= D(2,1) = (c_3\cos(q_2 + q_3) + l_2\cos(q_2)) + m_2(c_2\cos(q_2) + l_2\cos(q_2))\,,\\
D(1,3) &= D(3,1) = c_3m_3\cos(q_2 + q_3)\,,\\
D(2,2) &= I_{2z} + I_{3z} + c_2^2m_2 + c_3^2m_3 + I_2^2(m_2 + m_3) + 2c_2l_2m_2 + 2c_3l_2m_3\cos(q_3)\,,\\
D(2,3) &= D(3,2)m_3c_3^2 + l_2m_3\cos(q_3)c_3 + I_{3z}\,,\\
D(3,3) &= m_3c_3^2 + I_{3z}\,,
\end{aligned} \tag{46}$$

$$
\begin{aligned}
g(1,1) &= -g(m_1+m_2+m_3)\,, \\
g(2,1) &= -C_3 g m_3 \cos(q_2+q_3) - g(m_2(C_2+L_2)+L_2 m_3)\cos(q_2)\,, \\
g(3,1) &= -C_3 g m_3 \cos(q_2+q_3)\,.
\end{aligned} \tag{47}
$$

TABLE II

PLANT PARAMETERS TABLE

Parameter	Value	Units
m_1	21.29	Kg
m_2	8.57	Kg
m_3	2.33	Kg
I_2	0.435	$Kg-m^2$
I_3	0.062	$Kg-m^2$
d_0	0.5	m
L_2	0.425	m
L_3	0.527	m
C_2	-0.339	m
C_3	0.320	m
g	9.81	m/s^2